Are the physical properties of Xe@cryptophane complexes easily predictable? the case of *syn* and *anti* tris-*aza*-cryptophanes

Martin Doll, Patrick Berthault, Estelle Léonce, Céline Boutin, Thierry Buffeteau, Nicolas Daugey, Nicolas Vanthuyne, Marion Jean, Thierry Brotin, Nicolas de Rycke

Are the physical properties of Xe@Cryptophane complexes easily predictable? The case of the *syn* and *anti* tris-*aza*-cryptophanes

Martin Doll,[†] Patrick Berthault,[‡] Estelle Léonce,[‡] Céline Boutin,[‡] Thierry Buffeteau,[§] Nicolas Daugey,[§] Nicolas Vanthuyne,[&] Marion Jean,[&] Thierry Brotin,*[,†], Nicolas De Rycke,*[,†]

[†] Laboratoire de Chimie de l'ENS Lyon, (UMR 5182 CNRS-ENS-Université), Université Claude Bernard Lyon 1, F69342, Lyon, France

[‡] Université Paris-Saclay, CNRS, CEA, Nanosciences et Innovation pour les Matériaux, la Biomédecine et l'Energie (UMR 3685 CEA-CNRS), 91191, Gif-sur-Yvette, France

[§] Institut des Sciences Moléculaires (UMR 5255 - Université-CNRS), Université de Bordeaux, 351 Cours de la Libération, 33405 Talence, France

[&]Aix Marseille Université, Centrale Marseille, CNRS, iSm2 UMR 7313, 13397 Marseille, France

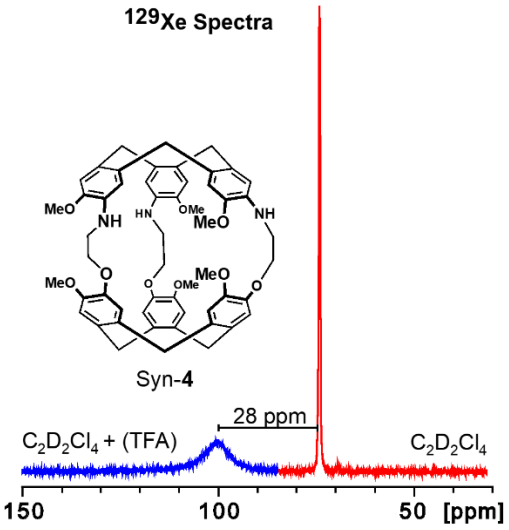

ABSTRACT: We report the synthesis and the optical resolution of C_3-symmetrical tris-*aza*-cryptophanes *anti*-**3** and *syn*-**4**, as well as the study of their interaction with xenon *via* hyperpolarized ^{129}Xe NMR. These molecular cages are close structural analogs of the two well-known cryptophane-A (**1**; chiral) and cryptophane-B (**2**; achiral) diastereomers since these new

compounds differ only by the presence of three nitrogen atoms grafted on the same cyclotribenzylene unit. The assignment of their relative (*syn* vs *anti*) and absolute configurations was made possible thanks to the combined use of quantum calculation at the DFT level and vibrational circular dichroism (VCD). More importantly, our results show that despite the large structural similarities with cryptophane-A (**1**) and -B (**2**), these two new compounds show very different behavior in the presence of xenon in organic solution. These results demonstrate that a prediction of the physical properties of the xenon@cryptophane complexes, only based on structural parameters, remains extremely difficult.

INTRODUCTION

Supramolecular structures based on poly-aromatic systems have attracted a lot of attention in the past and this area of research is still very active today. For instance, the pioneering work of Cram and co-workers in the 70-80's has been a source of inspiration to design new original structures capable of establishing very selective interaction with various substrates in solution.[1] In the same period, other organic systems such as cryptophane derivatives have emerged and this class of compound has been the subject of numerous studies due to their ability to reversibly encapsulate atoms or small molecules in solution.[2] Thus, cryptophane derivatives, which are hollow molecules with a characteristic globular shape, are among the first artificial organic systems able to isolate a guest molecule from the bulk. This property makes the identification of these complexes through NMR easier since the encapsulated guest molecule usually shows a specific spectral signature, which is different from the guest molecule in solution. Famous examples have been reported in the past with methane, xenon, or even cationic species as guests in which nuclei of the encapsulated species show large chemical shift difference with respect to the free guest present in the bulk.[3]

Despite the great interest for these supramolecular systems, cryptophane derivatives remain difficult to prepare and the production of novel structures remains limited even though sustained efforts have been made by our group and others to develop the chemistry of these molecules. Several issues related to the synthesis of these derivatives strongly limit the possibility to prepare easily new cryptophane derivatives. For example, ring-closure reactions leading to the formation of the two cyclotribenzylene units (CTB) are the main limitation, as the electron-donating substituents must be grafted onto the benzene rings for the reaction to be successful. Thus, for this reason the overwhelming majority of the cryptophane derivatives reported in the literature has been prepared from vanillyl alcohol as a starting material, a molecule that contains two oxygen atoms grafted on the benzene ring.[4] Despite the difficulties in preparing novel cryptophane structures decorated with heteroatoms, the synthesis of sulfur-containing cryptophanes has been reported by Hardie *et* al and Chambron *et* al via the *direct-coupling method*.[5] Interestingly, this approach does not require the formation of a CTB ring at a later stage of the synthesis but it cannot be easily extended to the synthesis of cryptophane derivatives bearing heteroatoms other than sulfur. Of course, the synthesis of heteroatom-decorated cryptophane derivatives can be considered, but their synthesis would require additional chemical transformations once the cryptophane backbone is formed, which remains a difficult task.

The synthesis of *aza*-congeners of cryptophane-A and cryptophane-B has not been reported yet. This may appear surprising since when grafted onto a benzene ring, nitrogen is a strong electron-donating atom and the formation of nitrogen-containing CTB derivatives has been reported with excellent yields.[6] Nevertheless, the replacement of one or several oxygen atoms present in the structures of cryptophane-A (**1**; chiral) or cryptophane-B (**2**; achiral) is not straightforward and it represents an interesting synthetic challenge. In this article, we focus exclusively on the synthesis of *aza*-cryptophane *anti*-**3** and *syn*-**4** bearing three nitrogen atoms

grafted on the same CTB cap (Chart 1). It is noteworthy that these new *aza*-derivatives *anti*-**3** and *syn*-**4** are both chiral compounds.

Cryptophane-A (**1**) and cryptophane-B (**2**) are diastereomers with small internal cavities (V_{vdw} = 90-100 Å^3) and they differ only by the arrangement of the three linkers (*anti* conformation for cryptophane-A and *syn* conformation for cryptophane-B).[7,8] Another way to describe these two systems is to assign for each CTB unit a stereo-descriptor *M* or *P*.[9] Thus, for the two structures reported in Chart 1, we can associate the *PP* absolute configuration (AC) for the cryptophane-A derivative whereas cryptophane-B possesses the *PM* absolute configuration. It is noteworthy that *anti*-cryptophane-A (**1**) and *anti*-**3** are not defined by the same stereo-descriptors (the same is true for *syn*-cryptophane-B (**2**) and *syn*-**4**). Indeed, the readers have to keep in mind that the stereo-descriptors used for compounds *anti*-**3** and *syn*-**4** are different from those used for the two cryptophane congeners A (**1**) and B (**2**) (Chart 1) due to the change of priority between the oxygen and nitrogen atoms.

Replacement of three oxygen atoms by nitrogen atoms is expected to modify both the electronic and magnetic properties of the cavity without affecting significantly the cavity size. Thus, even though compounds **3** and **4** are expected to be very similar in shape to compounds **1** and **2**, respectively, their molecular recognition properties are also expected to differ to some extent. Moreover, the introduction of nitrogen atoms allows us to investigate the binding properties of these hosts under different conditions. Indeed, protonation of the nitrogen atoms under acidic condition should affect significantly the properties of these two hosts.

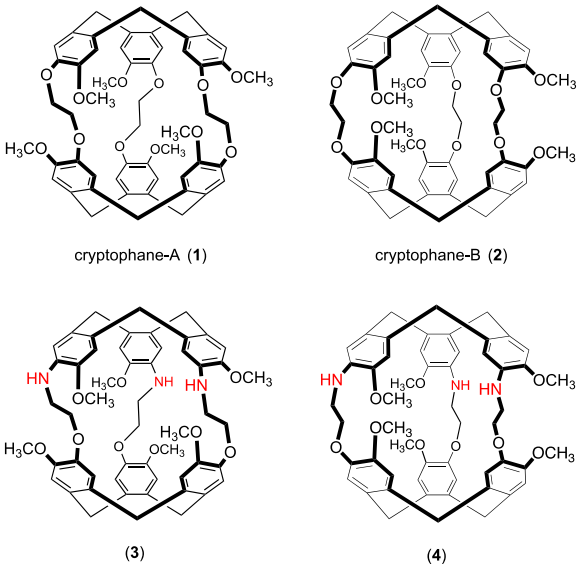

Chart 1: Chemical structures of cryptophane-A (**1**, chiral, D_3 symmetry), cryptophane-B (**2**; achiral, C_{3h} symmetry) and *aza*-cryptophane congeners (**3** and **4**; both chiral, C_3 symmetry). Only a single enantiomer is shown for chiral compounds, *PP*-**1**, *PM*-**2**, *PM*-**3** and *MM*-**4**.

We report in this article the synthesis and the characterization of the two *aza*-cryptophane *anti*-**3** and *syn*-**4**. The two enantiomers of compounds *anti*-**3** and *syn*-**4** were first separated by High-Performance Liquid Chromatography (HPLC) using chiral stationary phases. Then, the chiroptical properties of the optically active compounds *anti*-**3** and *syn*-**4** were investigated by Electronic Circular Dichroism (ECD) and Vibrational Circular Dichroism (VCD) in order to determine their relative and absolute configuration. Finally, the formation of their complexes with xenon in organic solution was reported under different conditions and these results were compared with those previously obtained for cryptophane-A (**1**) and cryptophane-B (**2**) in the same conditions.

RESULTS

Synthesis of *aza*-cryptophanes *anti*-3 and *syn*-4. The strategy used to prepare compounds **3** and **4** relies on the so-called *template method*, which allows the formation of the

two CTB caps of the cryptophane derivatives at different stages of synthesis.[2b] First, the preparation of a CTB decorated with three nitrogen atoms was performed using 4-amino-3-methoxybenzyl alcohol (**5**) as starting material, according to a known procedure (Scheme 1, route A).[10] This synthesis leads to the triamino-CTB **6** in three steps (acylation with acetic anhydride, cyclization and deprotection of the acetyl moieties), with a 62% overall yield. Finally, compound **6** was allowed to react with bromoacetyl bromide in the presence of DIPEA to give compound **7** in 55% yield. Thus, using route A compound **7** was obtained with a 34% overall yield but we noticed that the formation of compound **7** could be improved by using a two steps approach (Scheme 1, route B). In this novel approach, compound **5** was allowed to react with two equivalents of bromoacetyl bromide in presence of DIPEA to give compound **8** in 70% yield. In the presence of a $HClO_4$/AcOH mixture, compound **8** gave rise to compound **7** in 86% yield, leading to a shorter synthesis and a better overall yield (60%).

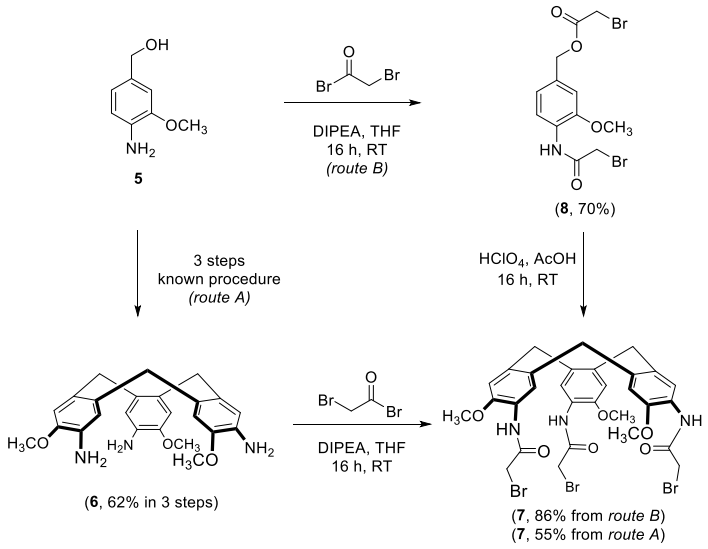

Scheme 1: Synthesis of tris-aza-CTB **7** according to route A (four steps) and route B (two steps).

Thanks to the presence of three terminal bromomethyl functions, compound **7** can be used as an interesting chemical platform to introduce new functionalities via S_N2 reactions. Thus, compound **7** was allowed to react with three equivalents of protected vanillyl alcohol **9** in the presence of K_2CO_3 to give compound **10** in moderate yield (52%) after purification

(Scheme 2). Then, transformation of the three aromatic amide functions of compound **10** into secondary aromatic amines was performed in THF, under reflux conditions, by using borane dimethyl sulfide complex as the reducing agent. Purification on silica gel gave rise compound **11** in moderate yield (38%). Finally, the second ring closure reaction was performed by using a mixture of perchloric acid and acetic acid at room temperature. Purification of the crude product on silica gel followed by recrystallization in CH_2Cl_2/EtOH allowed us to isolate two compounds. The first eluted compound was isolated with a yield of 1.2% and the second was isolated with a 6% yield. The analysis of their respective ^{1}H NMR spectra revealed proton signals characteristic of a cryptophane skeleton. These two ^{1}H NMR spectra show a lot of similarities suggesting that both compounds are *syn* and *anti*-cryptophane diastereomers. Indeed, the presence of four signals in the aromatic region of the ^{1}H NMR spectra allowed us to confirm that these two compounds have C_3-symmetry, as expected for *anti*-**3** and *syn*-**4**. Thanks to ^{1}H, ^{13}C and 2D-NMR (COSY, HSQC and HMBC) spectroscopy, the complete assignment of the ^{1}H signals of these two derivatives was carried out (Figures S1-S18). However, the relative configuration (*syn vs anti*) of the first and second eluted compounds is not known at this stage and additional characterizations are necessary to determine this point. In addition, compounds *anti*-**3** and syn-**4** both possess an inherent chiral structure due to their lack of symmetry (C_3 group). Thus, the combined use of vibrational circular dichroism (VCD) spectroscopy and density functional theory (DFT) calculations appeared here as the method of choice for the attribution of their relative and absolute configuration. Indeed, even though the two compounds show very similar structures, *anti*-**3** and *syn*-**4** should exhibit different VCD spectra, as already observed with optically active cryptophane-A congeners decorated with nine methoxy substituents.[11]

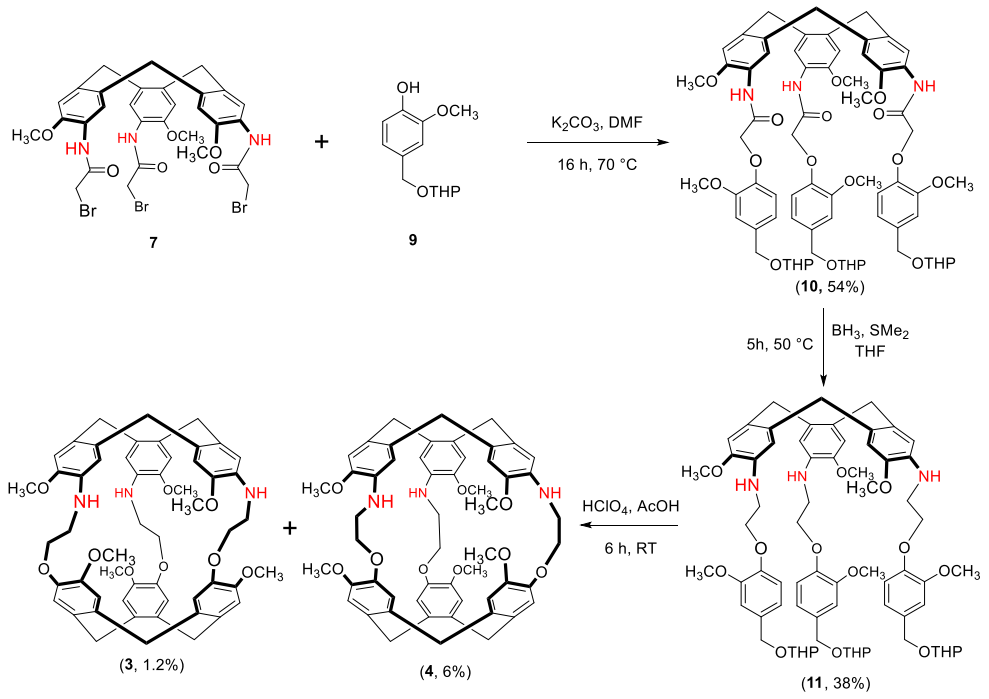

Scheme 2: Synthesis of aza-cryptophanes *anti*-**3** and *syn*-**4**.

Assignment of the relative and absolute configuration of 3 and 4. The two enantiomers of the first and second eluted cryptophanes on silica gel have been separated by HPLC using chiral stationary phase (Figures S19-S20). The two enantiomers of the first isolated cryptophane derivative on silica gel have been separated on Chiralpak IE chiral column. Each enantiomer of this derivative has been isolated with an enantiomeric excess (ee) >98%. Similarly, the two enantiomers of second eluted cryptophane on silica gel have been separated on the same chiral column but using a different mobile phase. These two enantiomers have also been isolated with excellent ee (>99.5%). In the two separations, sufficient material was isolated to study their chiroptical properties by VCD and ECD spectroscopy in order to determine their relative and absolute configuration. The ^{1}H NMR spectra of the enantiopure cryptophanes (+)-**3**, (–)-**3**, (+)-**4** and (-)-**4** are reported in Supporting Information (Figures S21-S24).

Specific Optical Rotation (SOR) values for the two enantiomers of compounds **3** and **4** have been measured in CH_2Cl_2 and compared to the SOR values of compound **1** (Figure S25). The first eluted enantiomer of **3**, [CD(–)$_{254}$]-**3**, exhibits negative values of SOR at 436, 546, 577

and 589 nm. Thus, the sign of the SOR value at 589 nm and the sign of the CD at 254 nm is the same, which facilitates its identification. The SOR values of [CD(−)$_{254}$]-**3** are very close than those measured for [CD(−)$_{254}$]-**1**. The first eluted enantiomer of **4**, [CD(−)$_{254}$]-**4**, shows also negative values of SOR at 436, 546, 577 and 589 nm, but these values are significantly lower than those measured for [CD(−)$_{254}$]-**3**.

The two enantiomers of the two compounds **3** and **4** were studied by IR and VCD spectroscopy. The IR spectra recorded in $CDCl_3$ of the first and second eluted compounds (silica gel) exhibit similar spectra in the spectral range 3600-950 cm^{-1}, and only small differences in the intensity of the IR bands are observed (Figures S26). Thus, it is not possible to assign the relative configuration (*syn* vs *anti*) of the two compounds from IR spectra. The VCD spectra recorded in $CDCl_3$ for the two enantiomers of compounds **3** and **4** are presented in Supporting Information (Figures S27-S28). For each compound, the VCD spectra of the two enantiomers are perfect mirror images, as expected for enantiopure compounds. Interestingly, a comparison of the VCD spectra of the two compounds reveals large spectral differences in the 1700-950 cm^{-1} region (Figure 1). For instance, the ν_{8b}C=C stretching vibration around 1610 cm^{-1} exhibits a negative band for the first eluted compound on silica gel and the second eluted enantiomer on Chiralpak IE column (Figure 1a, bottom), whereas the same stretching vibration shows a positive-negative bisignate band for the second eluted compound on silica gel and the first eluted enantiomer on Chiralpak IE column (Figure 1b, bottom). Likewise, the ν_{19b}C=C stretching vibration around 1510 cm^{-1} exhibit a negative-positive bisignate band in Figure 1a and a negative-positive-negative pattern in Figure 1b. More importantly are the spectral differences in the 1300-1200 cm^{-1} region. Ab-initio calculations of the VCD spectra at the DFT level (B3LYP/6.31G**) for the *PM-anti*-**3** and the *PP-syn*-**4** molecules allow us to reproduce with a good degree of confidence the experimental VCD spectra of the two compounds considered in Figure 1a and 1b, respectively, allowing the determination of their relative and

absolute configurations.[12] It can be concluded that the first eluted compound on silica gel corresponds to the *anti*-**3** derivative. In turn, the second eluted compound on silica gel can undoubtedly be attributed to the *syn*-**4** derivative. In addition, the comparison between the theoretical and experimental VCD spectra reveals that the *PM* (**or** *MP*) absolute configuration can be attributed to the second (or first) eluted enantiomer of *anti*-**3** on the Chiralpak IE column. For the derivative *syn*-**4**, the VCD experiments allow us to assign the *PP* (**or** *MM*) absolute configuration for the first (or second) eluted enantiomer on the chiral HPLC column. The chemical structures of these four compounds are reported in Supporting Information (Figure S29).

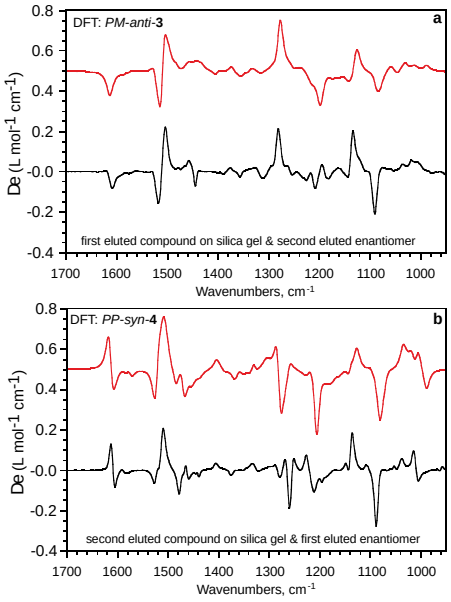

Figure 1: Experimental VCD spectra (bottom) of the first eluted compound on silica gel and the second eluted enantiomer on Chiralpak IE column (a) and of the second eluted compound on silica gel and the first eluted enantiomer on Chiralpak IE column (b) recorded in $CDCl_3$ at 25°C. Theoretical VCD spectra (top) for the *PP*-*anti*-**3** (a) and the *PP*-*syn*-**4** (b).

As compounds *PP*-**1** and *PM*-**3** show large structural similarities, it is interesting to compare their IR and VCD spectra in order to evaluate how the introduction of heteroatoms in the cryptophane-A skeleton can affect the vibrational spectra. Of course, this comparison cannot

be done with compounds *syn*-**4** and cryptophane-B (**2**) since compound **2** is not chiral. It can be noticed that the IR spectra of compounds *anti*-**1** and *anti*-**3** are very similar and the main spectral differences are observed below 1250 cm^{-1} (Figure S30). On the other hand, more important spectral differences are observed in their VCD spectra (Figure S31). Indeed, the overall intensity of the VCD spectrum of compound *PM*-**3** is measured with a significant lower intensity than its parent molecule *PP*-**1**, probably as a consequence of the breakdown of its molecular symmetry. Moreover, this spectrum reveals large spectral differences with respect to the VCD spectrum of *PP*-**1** in the 1400-1350 and 1250-1200 cm^{-1} region related to the linkers and associated with the wagging CH_2 chains and ν_aC-O-C stretching mode, respectively.

The ECD spectra of compounds have been recorded in CH_2Cl_2 and THF for compound *anti*-**3** and in CH_2Cl_2, $CHCl_3$, CH_3CN and THF for compound *syn*-**4** (Figures S32-S37). In CH_3CN the *MM*-syn-**4** enantiomer shows several positive-negative bands of different intensities between 220 and 340 nm (Figure S36). For instance, this enantiomer shows two negative Cotton bands of relatively high intensities at 292 nm ($\Delta\varepsilon = -12.6$ L mol^{-1} cm^{-1}) and 250 nm ($\Delta\varepsilon = -73.5$ L mol^{-1} cm^{-1}). Two positive Cotton bands of similar intensities are also observed for this enantiomer at 269.5 nm ($\Delta\varepsilon = +57.9$ L mol^{-1} cm^{-1}) and at 232 nm ($\Delta\varepsilon = +65.7$ L mol^{-1} cm^{-1}). In addition, a close examination of the ECD spectrum reveals the presence of additional Cotton bands of very week intensities at higher wavelengths. Indeed, the same enantiomer shows one negative Cotton band at 318 nm ($\Delta\varepsilon \sim -1.0$ L mol^{-1} cm^{-1}) and two positive Cotton bands at 328 nm and 306 nm ($\Delta\varepsilon \sim +2.0$ L mol^{-1} cm^{-1}). It is noteworthy that the *PP*-syn-**4** enantiomer shows a perfect mirror image in the same condition. Changing the nature of the solvent has little impact of the global shape of the ECD spectra except for the weak Cotton bands located between 300 and 340 nm.

Additional ECD experiments were performed in CH_2Cl_2 with the two enantiomers of *syn*-**4** in the presence of various amount of trifluoroacetic acid (TFA). For instance, compound *MM*-*syn*-**4** shows large spectral differences as the amount of TFA added to the CH_2Cl_2 solution increases. These spectral differences result in a significant decrease of all the Cotton bands observed between 230 and 300 nm (Figure S38a). The *PP*-*syn*-**4** enantiomer behaves similarly (Figure S38b). Under similar experimental conditions, we observed that the two enantiomers of *anti*-**3** are also affected by the addition of TFA into the solution (Figures S39 a,b). The corresponding spectra of anisotropy factors ($g = \Delta\varepsilon/\varepsilon$) were also calculated and are reported in Supporting Information (Figures S32-S39).

Study of the interaction of *anti*-3 and *syn*-4 with xenon using hyperpolarized ^{129}Xe NMR. Laser-polarized xenon prepared in the batch mode has been introduced in $C_2D_2Cl_4$ solutions containing compounds *anti*-**3** and *syn*-**4** and studied at 11.7 T and 293 K. The ^{129}Xe spectrum of xenon in the *anti*-**3** solution reveals two sharp signals that can be easily identified. The intense signal calibrated at $\delta = 223$ ppm (Figure 2a) corresponds to xenon dissolved in tetrachloroethane-d_2. The second signal, shifted toward low frequencies ($\delta = 51.9$ ppm), corresponds to xenon caged in the compound *anti*-**3**. Under the same experimental conditions, the ^{129}Xe NMR spectrum of *syn*-**4** is characterized by two sharp signals indicating that here also xenon experiences a slow *in-out* exchange dynamics with the compound *syn*-**4** at 293 K and 11.7 T (Figure 2b). In addition to the strong ^{129}Xe signal corresponding to xenon free in 1,1,2,2-tetrachloroethane-d_2, calibrated at 223 ppm, another sharp signal shifted towards low frequencies and located at $\delta = 72.1$ ppm corresponds to xenon caged in *syn*-**4**.

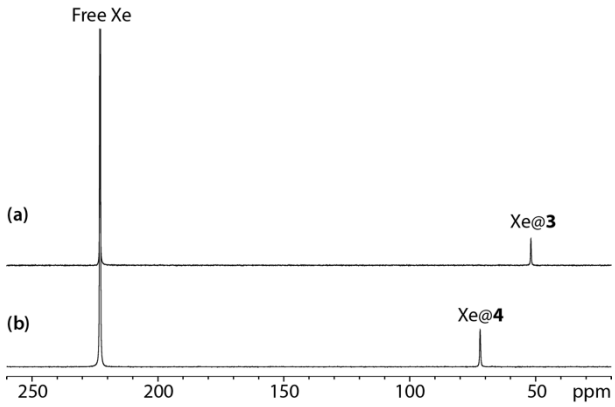

Figure 2: One-scan ^{129}Xe NMR spectra of (a) Xe@*anti*-**3** (c = 3.0 mM) and (b) Xe@*syn*-**4** (c = 3.3 mM) recorded in $C_2D_2Cl_4$ at 293 K and 11.7 T.

Since compounds *anti*-**3** and *syn*-**4** belong to the families of cryptophane-A (**1**) and B (**2**) respectively, it seems interesting to compare their ^{129}Xe NMR spectra in the same experimental conditions. The most significant difference is between the complexes with *syn*-**2** (cryptophane-B) and *syn*-**4**, the former giving rise to a fast *in-out* xenon exchange situation at 11.7 T and 293 K. Consequently, at this temperature its ^{129}Xe NMR spectrum does not exhibit a specific resonance frequency for the complex Xe@**2**.[8] Conversely, the ^{129}Xe NMR spectrum of a solution containing a mixture of cryptophanes *anti*-**3** and *anti*-**1** reveals three signals (Figure 3), indicating slow in-out xenon exchange for both complexes. The two high-field shifted ^{129}Xe NMR signals, at 65.9 and 51.9 ppm correspond to xenon encapsulated in compounds **1** and **3**, respectively. From the linewidths of the caged xenon signals, a clear difference in the *in-out* exchange dynamics of xenon can be observed between the two cryptophanes. This exchange is faster for the system Xe@**1** than for Xe@**3**. At first sight this may appear surprising since these compounds are structurally identical (only three oxygen atoms of **1** have been replaced by three nitrogen atoms) and possess similar cavity size. From this experiment it can be concluded that the presence of nitrogen atoms in the skeleton of the compounds *anti*-**3** and *syn*-**4** reduces significantly the xenon *in-out* exchange rate compared to what is observed with the corresponding cryptophanes containing ethylenedioxy linkers (*anti*-

1 and *syn*-**2**, respectively). The knowledge of the association constant for the Xe@**1** complex (3900 M^{-1}), allow us to estimate the association constant K_a = 2300 M^{-1} for the Xe@**3** complex. From a separate ^{129}Xe NMR experiment performed on the mixture of cryptophanes **3** and **4**, the association constant with **4** could be estimated to be 2800 M^{-1}. Keep in mind that a large uncertainty is encountered with these successive experiments (cumulative error).

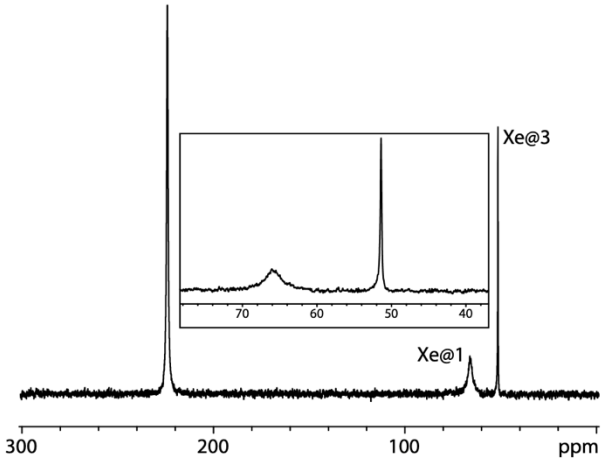

Figure 3: One-scan ^{129}Xe NMR spectrum of compound **3** (c =1.6 mM) and cryptophane-A (**1**) (c = 1.3 mM) recorded at 293 K in $C_2D_2Cl_4$.

Finally, we have studied the effect of protonation of the three aromatic amine moieties present in the cryptophane skeleton of *anti*-**3** and *syn*-**4** on their ^{129}Xe NMR spectra. The ^{129}Xe NMR spectra of Xe@*anti*-**3** and Xe@*syn*-**4** complexes have been recorded in $C_2D_2Cl_4$ solutions at 293 K with an excess of TFA. It can be seen that addition of 1 µL TFA to these solutions has a drastic effect on ^{129}Xe NMR spectra of both Xe@*anti*-**3** and Xe@*syn*-**4** complexes (Figures S40-S41). For instance, with addition of TFA the Xe@*syn*-**4** signal is low-field shifted to reach a value of 99.7 ppm ($\Delta\delta$ = 27.6 ppm with respect to neutral Xe@*syn*-**4** complex) and is broadened. More surprisingly, in the same conditions the Xe@*anti*-**3** complex gives rise to a very broad signal that is difficult to distinguish from noise on the ^{129}Xe NMR spectrum at 293 K.

DISCUSSION

Anti-**3** and *syn*-**4** aza-cryptophanes have been obtained in low yield and they have been more difficult to isolate than their congeners cryptophane-A and cryptophane-B due to the presence of nitrogen atoms in the cryptophane skeletons. It is noteworthy that the formation of *anti*-**3** and *syn*-**4** takes place during the same reaction whereas two different protocols are necessary to isolate cryptophane-A and cryptophane-B. At first sight, the difficulties to obtain compounds *anti*-**3** and *syn*-**4** may appear surprising since the synthetic pathway used to prepare these two derivatives is similar to the one used for the preparation of compounds *anti*-**1** and *syn*-**2**. Indeed, the second ring closing reaction involves only benzenic groups decorated with oxygen atoms and the CTB decorated with aromatic amine substituents does not directly participate to the cyclization reaction. Thus, the large difference in the isolated yields for these two compounds suggests that the protonation of the three nitrogen atoms has a strong impact on the conformation of the linkers, which in turn hinder the second ring closing reaction. Attempts have been made to improve the yield of the reaction by changing the experimental conditions. For instance, the replacement of $HClO_4$/AcOH by a $HClO_4$/MeOH mixture at room temperature also resulted in the formation of cryptophane *anti*-**3** and *syn*-**4** in small amount. The formation of these two diastereomeric compounds was detected by ^{1}H NMR spectroscopy but they were not isolated. A change of the nature of the acid did not allow us to improve the yield of the reaction. For instance, the use of a HCOOH/$CHCl_3$ (v: 1/1) mixture at 60°C under diluted conditions resulted in the formation of a complex mixture of compounds, which were not characterized, and the expected *syn* and *anti*-cryptophanes were not detected from the crude material. These conditions are those usually reported to produce in high yield the cryptophane-A (**1**) derivative and its congeners.[2] Similarly, the use of milder conditions did not allow us to

improve the yield of compounds *anti*-**3** and *syn*-**4**. For instance, the use of scandium triflate as Lewis acid has been reported to promote the ring closing reaction of many different systems such as cyclotriveratrylene, hemicryptophane and cryptophane derivatives.[13] Unfortunately, the use of this reagent in CH_2Cl_2 or in CH_3CN did not allow us to promote the formation of the two desired diastereomers. It should be noted that these experimental conditions were also used with the cryptophane precursor **10**, which can also be subjected to the Friedel-Crafts reaction under acidic conditions. In all cases, a complex mixture of compounds was observed and the analysis of the ^{1}H NMR spectrum of the crude mixture did not allow us to detect the desired compounds.

VCD spectroscopy associated with DFT calculations have been used to assign the relative (*anti* vs *syn*) and absolute configurations of compounds **3** and **4**. In contrast to cryptophane-A and B, among which only cryptophane-A is chiral, both cryptophane derivatives *anti*-**3** and *syn*-**4** are optically active and possess the same molecular C_3-symmetry. As the determination of the stereochemistry of each isolated cryptophane cannot be rapidly established from the analysis of their respective ^{1}H NMR, chiroptical techniques have been privileged in this article for the unambiguous determination of their stereochemistry. Previous studies performed on highly substituted cryptophane derivatives with C_3-symmetry have revealed that VCD and ROA spectra of *anti* and *syn* diastereomers displayed large spectral differences.[11,14] In these examples, DFT calculations (B3PW91/6-31G**) reproduced fairly well the main features of each spectrum, thus allowing to assign with a good degree of confidence the stereochemistry of each compounds.

As expected, compounds *anti*-**3** and *syn*-**4** show large spectral differences and DFT calculations (B3LYP/6-31G**) allow to reproduce fairly well these spectra. The main spectral differences between *anti*-**3** and *syn*-**4** concerns the VCD bands related to the C=C stretching vibrations (ν_{8b}C=C and ν_{19b}C=C around 1610 cm^{-1} and 1510 cm^{-1}, respectively) and those in the 1300-1200 cm^{-1} region related to alkyls chains and ν_aC-O-C stretching vibration. Thus, this

study allows the assignment of the *anti*-diastereomer to the first eluted compound on silica gel. In turn, the *syn*-diastereomer can be assigned to the second eluted compound. At first glance, this result is surprising considering that in the large majority of examples the cryptophane derivatives having the *anti*-stereochemistry are usually the major products. In this study, the *syn*-diastereomer is formed preferentially (6%) compared to its *anti*-congener (1.2%) even though the yield considered here are low. In addition, the comparison between the experimental and theoretical VCD spectra allows the assignment of the AC of each enantiomer of the two diastereomers. The *PM* (*MP*) absolute configuration has been attributed to the second (first) eluted enantiomer of *anti*-**3**, whereas the *PP* (*MM*) absolute configuration is related to the first (second) eluted enantiomer of *syn*-**4**.

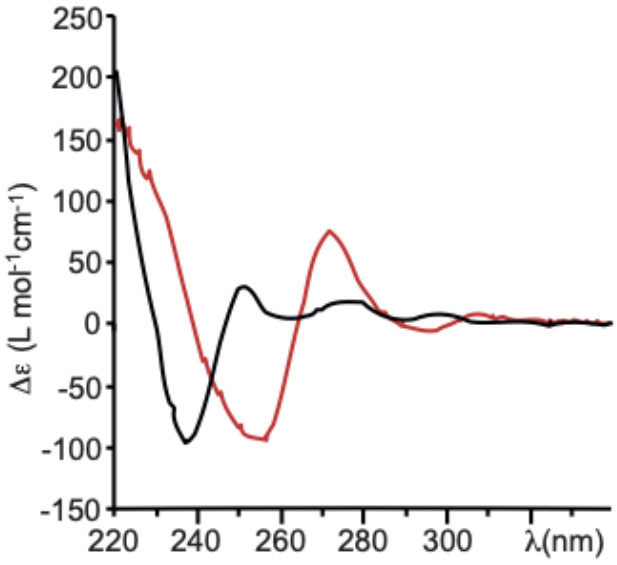

Figure **4**: ECD spectra of *anti-PM*-**3** (red spectrum) and *anti-PP*-**1** (black spectrum; cryptophane-A) derivatives recorded in THF at 298 K.

The ECD spectra of compound *anti-PM*-**3** reveal several spectral differences with respect the parent *anti-PP*-**1** derivative (Figure 4). These spectral differences come from the fact that three oxygen atoms of compound *anti*-**1** have been replaced by three nitrogen atoms. Indeed, this chemical modification has two important consequences. First, it leads to a

breakdown of the molecular symmetry with respect to the parent D_3-symmetric molecule **1**. The *anti*-**3** compound has C_3 symmetry and due to the excitonic coupling model, each Cotton band present on the ECD spectrum is the combination of several excited states whose number, position and intensity (defined by their rotational strength) are different from those observed with the *anti*-**1** compound having D_3 symmetry.[15] Second, the nitrogen atom attached to a benzene ring has a stronger electron-donating effect than an oxygen atom and, as a consequence, it causes a larger rotation of the electronic transitions moment for the excited states ^1L_b, ^1L_a and ^1B_b. Finally, in addition to these electronic effects, it cannot be excluded that the *anti*-**3** compound adopts different linker conformations compared to what is observed with cryptophane-A. These conformational changes may modify the shape of their ECD spectra.

The most interesting characteristics of *anti*-**3** and *syn*-**4** compounds derive from their molecular recognition properties with xenon. Indeed, these two compounds show behaviors very different from those observed with the parent molecules **1** and **2**. At first glance, these differences are difficult to interpret because compounds **1** and **3** on the one hand and, compounds **2** and **4** on the other hand, share great structural similarities. For instance, replacing C-O bonds by C-N bonds is not expected to change significantly the cavity size of compounds **3** and **4** compared to their parent derivatives. Our results reveal that xenon in the Xe@**3** and Xe@**4** complexes resonates in the same frequency region than the Xe@**1** complex. This is expected because the encapsulated xenon in compounds **1-4** is surrounded by six benzene groups decorated with electron-donating atoms (N, O for **3-4** and O, O for **1-2**). However, observation of the ^{129}Xe NMR spectra reveals that the replacement of three oxygen atoms by three nitrogen atoms has a strong effect on the *in-out* xenon exchange rate. In order to explain the large differences in behavior observed between hosts **3-4** and derivatives **1-2**, we assume that the aromatic amine groups can easily establish a hydrogen-bonding network with the residual water molecules. These water molecules may be present in compounds **3** and **4** before

doing the ^{129}Xe NMR experiments or they may come from the solvent $C_2D_2Cl_4$. In such an apolar solvent, the aromatic amine groups can favor the formation of a water cluster near the portal of cryptophanes **3**-**4**. It is noteworthy that the presence of water molecule within the cavity of cryptophane-A had already been identified in the solid state, however such encapsulation phenomenon could not be detected here with hosts **3**-**4** in $C_2D_2Cl_4$ solutions.[16] In this respect, ^{1}H NMR and ^{1}H-^{1}H NOESY spectra of host **4** recorded in $C_2D_2Cl_4$ both reveal a slow exchange between the free water signal at 1.6 ppm and a signal at 5.0 ppm which is assigned to clusters of water close to the cryptophane portals. (Figures S42-S43). Therefore, water molecules are likely to build a strong network of hydrogen bonds around the NH groups, which in turn can impact the *in-out* exchange dynamics of xenon. This result, which has not been observed with other cryptophane to date, sheds light on the possible role of water in the overall properties of the xenon-cryptophane complexes.

Herein, the most striking result comes from the analysis of the ^{129}Xe NMR spectrum of *syn*-**4** that shows a very sharp spectral signature whereas no signal corresponding to the Xe@**2** complex could be detected under the same experimental conditions (fast *in-out* exchange at the NMR time scale). Surprisingly, it can be noticed that the Xe@**3** and Xe@**4** complexes share more similarities with the Xe@cryptophane-111 complex that possesses a smaller inner cavity (V = 81 Å^3) and a large affinity for xenon in the same conditions.[17]

It is noteworthy that upon acidification with trifluoroacetic acid a drastic change of the ^{129}Xe NMR spectra is observed. Indeed, upon acidification the electron donor properties of the aromatic amine groups can be easily reversed and transformed into a strong electron attractor. This should interfere with xenon complexation by cryptophanes **3**-**4**. The acidification of the medium has a strong effect on the shape of the signal of the encapsulated xenon and it results in an increase of the exchange dynamics of xenon for the two complexes Xe@*anti*-**3** and Xe@*syn*-**4**. Even though, this effect is difficult to explain in details it is reasonable to assume

that the protonation of the three aromatic amine moieties has an effect on the conformation of the three linkers. Such hypothesis is also supported by the strong modifications observed for ECD spectra of hosts **3-4** upon acidification of the bulk which reveals potential significant conformational changes. Protonation of the nitrogen atoms may also destroy the water cluster present around hosts **3-4**. Both parameters may affect drastically the *in-out* exchange dynamics of xenon.

The large difference in the behavior of the cryptophane-A and cryptophane-B congeners in the presence of xenon rise some comments. The two examples cited in this article reveal that very slight change in the chemical structure of the cryptophane skeleton can have a tremendous effect on the overall physical properties of the Xe@cryptophane complexes. Thus, the study of cryptophanes **3** and **4** in the presence of xenon shows that the physical properties of the Xe@cryptophane complexes are difficult to predict accurately on the sole basis of the chemical structure of the studied cryptophane.

These results may have important consequences in the design of cryptophane biosensors for ^{129}Xe MRI applications. Pines and co-workers have shown that encapsulated xenon in cryptophane cavities could be used as a molecular tracer for the detection of biological events at the molecular level using hyperpolarized ^{129}Xe NMR.[18] Since then, many different molecular systems have been developed by our group and others to detect biomolecules or analytes by this means.[19] So far, the overwhelming majority of organic systems cited in the literature use the cryptophane-A skeleton to build up these biosensors.[20] A modification of the cryptophane backbone structure to improve the characteristics of these biosensors is desired to improve solubility in physiological media, the xenon binding constant or more importantly the xenon *in-out* exchange dynamics that plays a key role in the detection of these molecular tracers.[21] This work demonstrates that the main characteristics of the Xe@cryptophane complexes cannot be easily predicted based on structural parameters. Therefore, this may complicate the design of

new molecular tracers optimized for MRI application. On the other hand, quantum calculations can be used to predict some characteristic of these supramolecular complexes. For instance, this approach has been successfully used to predict precisely the chemical shift of the encapsulated xenon in cryptophane-111 derivatives decorated with a different number of hydroxyl functions.[22] However, a prediction of the physical properties of xenon present within cryptophane cavities is a difficult and time demanding task. For instance, the accurate prediction of ^{129}Xe properties inside molecular hosts requires the use of particular functionals~~-~~ density methods to take into account the dispersion energy to describe the host-guest interaction and relativistic effects have also to be included in the calculation in the case of xenon. In addition, it is noteworthy that a prediction of the *in-out* xenon exchange dynamics cannot be achieved by quantum calculations methods. The results reported in this article also suggest that the solvent and especially water has to be taken into consideration in these calculations to predict accurately the physical properties of these supramolecular systems.

CONCLUSION

We report the synthesis of two cryptophane-A and B congeners decorated with nitrogen atoms. The introduction of these heteroatoms yields to a breakdown of the molecular symmetry and, as a consequence, both compounds show an inherent chiral structure. The identification of the relative and absolute configurations of compounds *anti*-**3** and *syn*-**4** has been established thanks to the combined use of DFT calculations and VCD spectroscopy. As a result of the replacement of three oxygen atoms in compound *anti*-**1**, the new chiral compound *anti*-**3** exhibits very different chiroptical properties from those observed with cryptophane-A.

Interestingly, these new derivatives show remarkable features in organic solution in the presence of hyperpolarized xenon and large differences are observed in their ^{129}Xe NMR

spectra compared to those obtained with the cryptophane-A (**1**) and cryptophane-B (**2**) derivatives. For instance, both complexes Xe@**3** and Xe@**4** complexes exhibit very sharp ^{129}Xe NMR signals, which are characteristic of a slow *in-out* exchange dynamics of xenon. On the other hand, this exchange appears to be much faster in the case of cryptophane-A and cryptophane-B than for compounds *anti*-**3** and *syn*-**4** whereas the structures of these compounds are similar. Interestingly, we show that the *in-out* exchange dynamics of xenon of the Xe@**3** and Xe@**4** complexes can be modified upon acidification of the bulk by addition of TFA. The new derivatives **3** and **4** share structural similarities with cryptophane A and B, respectively, but their behavior in the presence of xenon reveals large differences, suggesting that a prediction of the physical properties of these complexes remains difficult on the basis of structural comparisons alone. In addition, the unusual characteristics observed with Xe@**3** and Xe@**4** complexes suggest a possible role of water molecules in the behavior of these complexes. Work is underway to understand how water molecules interact with cryptophane derivatives.

EXPERIMENTAL DETAILS

Mass spectra (HRMS) were performed by the Centre de Spectrométrie de Masse, University of Lyon. Analyses were performed with a hybrid quadrupole-time-of-flight mass spectrometer, microToF QII equipped with an electrospray ion source. Data Analysis 4.0 was used for instrument control, data collection, and data treatment. HRMS analyses were performed in full scan MS with a mass range from 50 to 2000 Da at an acquisition rate of 1 Hz. Transfer parameters were as follows: RF Funnel 1, 200 V; RF Funnel 2, 200 V; hexapole, 50 V; transfer time, 70 μs; and PrePulse storage time, 1 μs. Before each acquisition batch, external calibration of the instrument was performed with a sodium formate clusters solution. ^{1}H and ^{13}C NMR spectra were recorded at 300 or 400 and 75.5 or 100.6 MHz, respectively. Chemical shifts are referenced to Me_4Si (^{1}H, ^{13}C). Structural assignments were made with additional

information from gCOSY, gHSQC, and gHMBC experiments. Column chromatographic separations were carried out over Merck silica gel 60 (0.040−0.063 mm). Analytical thin-layer chromatography (TLC) was performed on Merck silica gel TLC plates, F-254. The solvents were distilled prior to use: DMF and CH_2Cl_2 from CaH_2, THF from Na/benzophenone, and pyridine from KOH.

HPLC Separation. The two enantiomers of *anti*-**3** were separated on semi-preparative Chiralpak IE (250 x 10 mm) chromatographic column. A mixture of EtOH + Et_3N (0.1% v/v)/CH_2Cl_2 (50/50) was used as a mobile phase (flow-rate = 5 mL/min). UV detection was performed at 254 nm. The two enantiomers of *anti*-**3** have been successfully separated with an enantiomeric purity > 98%. Similarly, the two enantiomers of *syn*-**4** were separated on semi-preparative Chiralpak IE (250 x 10 mm) chromatographic column. A mixture of Hexane/EtOH + Et_3N (0.1% v/v)/CH_2Cl_2 (10/40/50) was used as a mobile phase (flow-rate = 5 mL/min). UV detection was performed at 254 nm. The two enantiomers of *syn*-**4** have been successfully separated with an enantiomeric purity > 99.5%.

UV-visible and ECD spectroscopy. ECD spectra were recorded in CH_2Cl_2, $CHCl_3$, CH_3CN and THF at 293 K. Quartz cell with a path length of 0.2 cm and 1 cm were used for the ECD and UV-visible experiments. A concentration range of 8×10^{-5} to 1×10^{-4} moles per liter were used for ECD and UV-visible experiments. The ECD spectra were recorded in the wavelength range of 225 – 400 nm with a 0.5 nm increment and a 1 s integration time. The spectra were processed with standard spectrometer software. A smoothing procedure was applied by using a third-order least-square polynomial fit when necessary.

^{129}Xe NMR spectroscopy. Xenon enriched at 83% in isotope 129 was hyperpolarized via Spin Exchange Optical Pumping in the batch mode, using our home-built setup described.[23] The cryptophanes were solubilized in tetrachloroethane-d_2 and placed in 5-mm NMR tubes

capped with J. Young's valves. The transfer of hyperpolarized xenon into these tubes previously evacuated was made through a vacuum line in the fringe field of the NMR magnet. All the ^{129}Xe NMR experiments were run at 11.7 T and 293 K.

VCD Spectroscopy and DFT calculations. The IR and VCD spectra were recorded with a FTIR spectrometer equipped with a VCD optical bench, following the experimental procedure previously published.[24] Samples were held in a 250 μm path length cell with BaF_2 windows. IR and VCD spectra of the two enantiomers of *anti*-**3** and *syn*-**4** were measured in $CDCl_3$ at a concentration of 15 mM.

All DFT calculations were carried out with Gaussian 09.[25] Preliminary conformer distribution search of *anti*-**3** and *syn*-**4** was performed at the molecular mechanics level of theory, employing MMFF94 force fields incorporated in ComputeVOA software package. Around thirty conformers within roughly 2 kcal/mol of the lowest energy conformer were kept and further geometry optimized at the DFT level using B3LYP functional and 6-31G** basis set. Finally, only the four lowest energetic geometries were kept to predict the IR and VCD spectra of *anti*-**3** and *syn*-**4**. The four selected conformers exhibited a *gauche,gauche,gauche* conformations of the three linkers of *anti*-**3** and *syn*-**4**. Vibrational frequencies, IR and VCD intensities were calculated at the same level of theory. For comparison to experiment, the calculated frequencies were scaled by 0.97 and the calculated intensities were converted to Lorentzian bands with a full-width at half-maximum (FWHM) of 14 cm^{-1}.

EXPERIMENTAL PROCEDURE

Precursor 8. A solution of amine **5** (1.00 g, 6.54 mmol) in dry THF (30 mL) was set under an argon atmosphere and cooled to 0 °C with an ice bath. DIPEA (2.8 mL, 16.3 mmol) and bromoacetyl bromide (1.4 mL, 16.3 mmol) were added dropwise to the solution, which was

stirred at room temperature overnight. The originally pale-yellow solution turned into a brown suspension. Water (100 mL) was added to the mixture, which was extracted three times by EtOAc (3 x 100 mL). The organic layers were dried over sodium sulfate and the solvent was evaporated under reduced pressure. The crude was purified using column chromatography (SiO_2, eluent: CH_2Cl_2) to gain **8** as a beige powder (1.8 g, yield: 70%). ^{1}H NMR (300 MHz, $CDCl_3$, 25 °C): δ 8.80 (s, 1H), 8.32 (d, 1H, J = 8.2 Hz), 6.97 (dd, 1H, J = 1.6 Hz, J = 8.2 Hz), 6.92 (d, 1H, J = 1.6 Hz), 5.17 (s, 2H), 4.02 (s, 2H), 3.93 (s, 3H), 3.87 (s, 2H). ^{13}C{^{1}H} NMR (75 MHz, $CDCl_3$, 25 °C): δ 167.1, 163.3, 148.3, 131.4, 127.2, 121.3, 119.5, 110.3, 67.8, 56.0, 29.6, 25.8. HRMS (ESI) m/z: $[M+Na]^+$calcd for $C_{12}H_{13}Br_2NNaO_4$ 415.9104; found 415.9102.

***Aza*-CTB derivative 7.** Perchloric acid (50 mL) was added dropwise at room temperature to a solution of compound **8** (4.30 g, 10.8 mmol) dissolved in acetic acid (25 mL) under argon atmosphere. A white precipitate appeared within 30 minutes after the addition. The reaction mixture was stirred at room temperature for additional 16 hours. Then the mixture was poured into water (200 mL). The solid was filtered and washed three times with water (3 x 20 mL), twice with ethanol (2 x 20 mL) and twice with Et_2O (2 x 20 mL). After drying in vacuo, compound **7** was collected as a white solid (2.37 g, 86%). ^{1}H NMR (300 MHz, DMSO-d_6, 25 °C): δ 9.46 (s, 3H), 8.04 (s, 3H), 7.00 (s, 3H), 4.78 (d, 3H, J = 13.4 Hz), 3.83 (s, 9H), 3.56 (d, 3H, J = 13.3 Hz). ^{13}C{^{1}H} NMR (75 MHz, DMSO-d_6, 25 °C): δ 165.2 (3C), 148.7 (3C), 136.9 (3C), 131.6 (3C), 125.4 (3C), 123.7 (3C), 112.7 (3C), 56.1 (3C), 35.8 (3C), 30.8 (3C). HRMS (ESI) m/z: $[M+Na]^+$ calcd for $C_{30}H_{30}Br_3N_3NaO_6$ 787.9577; found 787.9541.

***Aza*-CTB derivative 10.** Compound **7** (2.00 g, 2.60 mmol) and potassium carbonate (4.0 g, 29 mmol) were suspended in dry DMF (50 mL). A solution of precursor **9** (2.4 g, 10 mmol) in dry DMF (10 mL) was added. The mixture was heated to 70 °C (oil bath) for 16 h. After cooling down to room temperature, water (300 mL) was added to precipitate the product, which was filtered, washed with water (3 x 40 mL) and Et_2O (40 mL) and dried under reduced

pressure. Compound **10** was obtained as a poorly soluble slight brown powder (1.73 g, 54%). ^{1}H NMR (400 MHz, $CDCl_3$, 25 °C): δ 9.09 (s, 3H), 8.43 (s, 3H), 7.01-6.84 (m, 12H), 4.78 (d, 3H, *J* = 13.6 Hz), 4.76-4.40 (m, 15H), 3.95-3.85 (m, 21H), 3.65 (d, 3H, *J* = 13.4 Hz), 3.54 (m, 3H), 1.95-1.45 (m, 18H). ^{13}C{^{1}H} NMR (101 MHz, $CDCl_3$, 25 °C): δ 166.4 (3C), 149.9 (3C), 147.3 (3C), 146.6 (3C), 135.6 (3C), 133.3 (3C), 131.2 (3C), 125.4 (3C), 121.0 (3C), 120.5 (3C), 115.3 (3C), 112.1 (3C), 111.7 (3C), 97.7 (3C), 69.8 (3C), 68.6 (3C), 62.3 (3C), 56.0 (3C), 55.9 (3C), 36.5 (3C), 30.6 (3C), 25.5 (3C), 19.5 (3C). HRMS (ESI) m/z: $[M+Na]^+$ calcd for $C_{69}H_{81}N_3NaO_{18}$ 1262.5407; found 1262.5413.

***Aza*-CTB derivative 11.** Triamide CTB **10** (4.51 g, 3.64 mmol) was suspended in THF (140 mL) and the mixture was stirred under an argon atmosphere. The solution was cooled down to 0 °C with an ice bath and borane dimethyl sulfide (15 mL of a 2 M solution in THF) was added dropwise to the suspension. The mixture was then heated to 50 °C (oil bath) for 3 hours. The remaining borane was quenched with methanol and the solvents were evaporated under reduced pressure. Water (200 mL) and DCM (200 mL) were added to the residue. The aqueous layer was extracted twice with dichloromethane (2 x 100 mL). The combined organic layers were dried on anhydrous sodium sulfate and the solvent was evaporated under reduced pressure. The crude was purified using column chromatography (SiO_2, eluent: EtOAc - petroleum ether (8:2)) to give rise to compound **11** (1.65 g, 38%) as a glassy product. ^{1}H NMR (400 MHz, $CDCl_3$, 25 °C): δ 6.93-6.80 (m, 9H), 6.71 (s, 3H), 6.62 (s, 3H), 4.73 (d, 3H, J = 13.6 Hz), 4.71 (d, 6H, *J* = 11.7 Hz), 4.43 (d, 6H, *J* = 11.7 Hz), 4.18 (m, 6H), 3.95-3.86 (m, 3H), 3.85 (s, 9H), 3.69 (s, 9H), 3.57-3.78 (m, 9H), 3.47 (d, 3H, *J* = 13.8 Hz), 1.92-1.48 (m, 18H). ^{13}C{^{1}H} NMR (101 MHz, $CDCl_3$, 25 °C): δ 149.6 (3C), 147.6 (3C), 145.8 (3C), 136.2 (3C), 132.4 (3C), 131.6 (3C), 128.1 (3C), 120.5 (3C), 113.9 (3C), 111.9 (3C), 111.3 (3C), 111.2 (3C), 97.5 (3C – double signal assigned to diastereoisomers), 77.2 (3C), 68.6 (3C), 68.1 (3C), 62.2 (3C), 55.8

(3C), 55.5 (3C), 43.1 (3C), 36.5 (3C), 30.5 (3C), 25.4 (3C), 19.4 (3C). HRMS (ESI) m/z: $[M+H]^+$ calcd for $C_{69}H_{88}N_3O_{15}$ 1198.6210; found 1198.6198.

***Aza*-cryptophane *anti*-3 and *syn*-4.** To a mixture of acetic acid (600 mL) and perchloric acid (200 mL) under an argon atmosphere, was added dropwise (12 hours) a solution of the cryptophane precursor **11** (8.0 g, 6.67 mmol) in acetic acid (200 mL). After the end of the addition, the mixture was further stirred for 6 hours and poured into water (1 L). The product was extracted with CH_2Cl_2 (2 x 1 L) and the organic layer was washed with water then with a saturated solution of Na_2CO_3 to remove traces of perchloric acid. The organic layer was dried over sodium sulfate and the solvent was evaporated under vacuum. Two cryptophane derivatives were identified by ^{1}H NMR spectroscopy from this crude product. These two compounds were separated by column chromatography on silica gel.

The first eluted product was identified as the compound *anti*-**3**. In order to isolate this diastereomer, the reaction described above was repeated three times. The crude product was purified on silica gel (CH_2Cl_2 88% - acetone 12%). The different fractions were evaporated by rotatory evaporation to give a product, which was precipitated in Et_2O. Recrystallisation in CH_2Cl_2/ethanol to give rise to *anti*-**3** (205 mg, 1.2%) as a beige solid. mp 220°C (decomp); ^{1}H NMR (400 MHz, $CDCl_3$, 25 °C): δ 6.72 (s, 3H), 6.67 (s, 3H), 6.54 (s, 3H), 6.35 (s, 3H), 4.60 (d, 3H, J = 13.5 Hz), 4.57 (d, 3H, J = 13.5 Hz,), 4.26-4.21 (m, 1H), 4.00-3.95 (m, 3H), 3.79 (s, 9H), 3.77 (s, 9H), 3.38-3.33 (m, 6H), 3.37 (d, 3H, J = 13.9 Hz), 3.30 (d, 3H, J = 13.8 Hz). ^{13}C{^{1}H} NMR (101 MHz, $CDCl_3$, 25 °C): δ 149.2 (3C), 146.4 (3C), 146.3 (3C), 136.2 (3C), 133.5 (3C), 132.3 (3C), 131.4 (3C), 128.7 (3C), 121.7 (3C), 114.2 (3C), 113.0 (3C), 111.4 (3C), 70.1 (3C), 55.7 (3C), 55.3 (3C), 44.4 (3C), 36.3 (3C), 36.0 (3C). UV (THF) λ (log ε) 310 nm (3.7, shoulder), 287 nm (4.15), 229 nm (4.85). HRMS (ESI) m/z: $[M+H]^+$ calcd for $C_{54}H_{58}N_3O_9$

892.4168; found 892.4164. Rf (DCM - acetone (85:15)): 0.55. (-)-*MP*-*anti*-**3'**, $[\alpha]_D^{25}$ = - 230.7 (*c* = 0.26, CH_2Cl_2); (+)-*PM*-*anti*-**3'**, $[\alpha]_D^{25}$= + 222.3 (*c* = 0.21, CH_2Cl_2).

The second eluted product was identified as the *syn*-**4** compound. It was purified on silica gel (CH_2Cl_2 85%- acetone 15%). It was then precipitated in Et_2O and recrystallized in dichloromethane/ethanol to give rise to a beige solid (330 mg, 6%), which was identified as the *syn*-**4** derivative. mp 180°C (decomp); ^{1}H NMR (400 MHz, $CDCl_3$, 25 °C): δ 6.75 (s, 3H), 6.62 (s, 3H), 6.52 (s, 3H), 6.36 (s, 3H), 4.60 (d, 6H, *J* = 13.8 Hz), 4.15 (d, 3H, *J* = 9,6 Hz,), 3.79 (s, 9H), 3.74 (s, 9H), 3.58-3.36 (m, 9H), 3.40 (d, 3H, *J* = 13.8 Hz) 3.30 (d, 3H, *J* = 13.8 Hz). ^{13}C{^{1}H} NMR (101 MHz, $CDCl_3$, 25 °C): δ 149.8 (3C), 147.7 (3C), 146.7 (3C), 136.5 (3C), 134.0 (3C), 132.3 (3C), 131.4 (3C), 128.3 (3C), 120.8 (3C), 112.9 (3C), 112.2 (3C), 112.1 (3C), 71.2 (3C), 55.9 (3C), 55.7 (3C), 43.5 (3C), 36.6 (3C), 36.4 (3C). UV (THF) λ (log ε) 315 nm (4.04; shoulder), 296 nm (4.2), 255 nm (4.45, shoulder). HRMS (ESI) m/z: $[M+H]^+$ calcd for $C_{54}H_{58}N_3O_9$ 892.4168; found 892.4188. Rf (DCM - acetone (85:15)): 0.4. (-)-*PP*-**1**, $[\alpha]_D^{25}$ = - 42.0 (*c* = 0.29, CH_2Cl_2); (+)-*MM*-**1**, $[\alpha]_D^{25}$ = + 45.2 (*c* = 0.30, CH_2Cl_2).

Supporting Information. ^{1}H and ^{13}C spectra of compounds **3**-**4**, **7**-**8** and **10**-**11**. Analytical HPLC of compound *anti*-**3** and *syn*-**4**. ^{1}H NMR spectra of compounds (-)-*MP*-**3**, (+)-*PM*-**3,** (-)-*PP*- **4** and (+)-*MM*-**4.** Optical rotations of compounds (-)-*MP*-**3**, (+)-*PM*-**3,** (-)-*PP*- **4** and (+)-*MM*-**4.** IR and VCD spectra of (+)-*PP*-**1** and (+)-*PM*-**3**. ECD spectra of compounds (-)-*MP*-**3**, (+)-*PM*-**3,** (-)-*PP*- **4** and (+)-*MM*-**4.** One-scan ^{129}Xe NMR spectra of compounds *anti*-**3** and *syn*-**4**. Geometries of *anti*-**3** and *syn*-**4** conformers used for IR/VCD spectra calculations.

AUTHOR INFORMATION

Corresponding author

*E-mail: thierry.brotin@ens-lyon.fr; nicolas.de-rycke@ens-lyon.fr

ORCID

Thierry Brotin: 0000-0001-9746-4706

Nicolas De Rycke: 0000-0001-6487-1030

Patrick Berthault: 0000-0003-4008-2912

Thierry Buffeteau: 0000-0001-7848-0794

Nicolas Vanthuyne: 0000-0001-7848-0794

Martin Doll: 0000-0001-9254-1821

Notes

The authors declare no competing financial interest.

ACKNOWLEDGEMENTS

The French National Research Agency (ANR) is acknowledged for financial support (Project ANR19-CE19-0024 PHOENIX).

(1) a) Cram, D. J.; Cram, J. M. Host-Guest Chemistry. Complexes Between Organic Compounds Simulate the Substrate Selectivity of Enzymes. *Science*, **1974**, *183*, 803-809. b) Cram, D. J.; Cram, J. M. Design of Complexes Between Synthetic Hosts and Organic

Guests. *Account of Chem. Res.* **1978**, 8-14. c) Chao, Y.; Weisman. G. R.; Sogah, G. D. Y.; Cram. D. J. Host Guest Complexation. 21. Catalysis and Chiral Recognition through Designed Complexation of Transition States in Transacylations of Amino Ester Salts. *J. Am. Chem. Soc.* **1979**, *101*, 4948-4958. d) Cram. D. J. The Design of Molecular Host, Guest, and their Complexes. *Science*, **1988**, *240*, 760-767.

(2) a) Collet, A. Cyclotriveratrylene and Cryptophane. *Tetrahedron*, **1987**, *4*, 24, 5725-5759. b) Brotin, T.; Dutasta, J.-P. Cryptophanes and their Complexes: Present and Future. *Chem. Rev.* **2009**, *109*, 88-130.

(3) a) Garel, L.; Dutasta, J.-P.; Collet, A. Complexation of Methane and Chlorofluorocarbons by Cryptophane-A in Organic Solution. *Angew. Chem. Int. Ed.* **1993**, *32*, 1169-1171. b) Bartik, K.; Luhmer, M.; Dutasta, J.-P.; Collet, A.; Reisse, J. ^{129}Xe and ^{1}H NMR Study of the Reversible Trapping of Xenon by Cryptophane-A in Organic Solution. *J. Am. Chem. Soc.* **1998**, *120*, 784-791. c) Brotin, T.; Montserret, R.; Bouchet, A.; Cavagnat, D.; Linares, M.; Buffeteau, T. High Affinity of Water-Soluble Cryptophanes for Cesium Cation. *J. Org. Chem.* **2012**, *77*, 1198-1201.

(4) See for instance: a) Baydoun, O.; De Rycke, N.; Léonce, E.; Boutin, C.; Berthault, P.; Jeanneau, E.; Brotin, T. Synthesis of Cryptophane-223 Type Derivatives with Dual Functionalization. *J. Org. Chem.* **2019**, *84*, 9127-9137. b) Dubost, E.; Kotera, N.; Garcia-Argote, S.; Boulard, Y.; Léonce, E.; Boutin, C.; Berthault, P.; Dugave, C.; Rousseau, B. Synthesis of a Functionalizable Water-Soluble Cryptophane-111. *Org. Lett.* **2013**, *15*, 2866-2868. c) Taratula, O.; Hill, P. A.; Khan, N. S.; Dmochowski, I. J. Shorter Synthesis of Trifunctionalized Cryptophane-A Derivatives. *Org. Lett.* **2011**, *13*, 1414-1417. d) Wong, T-H.; Chang, J-C.; Lai, C-C.; Liu, Y-H. ; Peng, S-M. ; Chiu, S-H. Hemicarceplexes Modify the Solubility and Reduction Potentials of C_{60}. *J. Org. Chem.* **2014**, *79*, 3581-3586.

(5) a) Little, M. A.; Donkin, J.; Fisher, J.; Halcrow, M. A.; Loder, J.; Hardie, M. J. Synthesis and Methane-Binding Properties of Disulfide-Linked Cryptophane-0.0.0. *Angew. Chem. Int. Ed.* **2012**, *51*, 764-766. b) Brégier, F.; Lavalle, J.; Chambron, J.-C. Capping α-Cyclodextrin with Cyclotriveratrylene by Triple Disulfide-Bridge Formation. *Eur. J. Org. Chem.* **2013**, *13*, 2666-2671.

(6) Bohle, D. S.; Stasko, D. J. Salicylaldiminato Derivatives of Cyclotriveratrylene: Flexible Strategy for New Rim-Metalated CTV Complexes. *Inorg. Chem.* **2000**, *39*, 5768-5770.

(7) Gabard, J.; Collet, A. Synthesis of a (D_3)-Bis(cyclotriveratrylenyl) Macrocage by Stereospecific Replication of a (C_3)-Subunit. *J. Chem. Soc. Chem. Comm.* **1981**, 1137-1139.

(8) Brotin, T.; Jeanneau, E.; Berthault, P.; Léonce, E.; Pitrat, D.; Mulatier, J.-C. Synthesis of Cryptophane-B: Crystal Structure and study of its complex with Xenon. *J. Org. Chem.* **2018**, *83*, 14465-14471.

(9) a) IUPAC Tentative Rules for the Nomenclature of Organic Chemistry. Section E. Fundamental Stereochemistry. *J. Org. Chem.* **1970**, *35*, 2849-2867. b) Collet, A.; Gabard, G.; Jacques, J.; Césario, M.; Guilhem, J.; Pascard, C. Synthesis and Absolute Configuration of Chiral (C_3) Cyclotriveratrylene Derivatives. Crystal Structure of (*M*)-(-)2,7,12-Triethoxy-3,8,13-tris-[(*R*)-1-methoxycarbonylethoxy]-10,15-dihydro-5*H*-tribenzo[*a*,*d*,*g*]-cyclononene. *J. Chem. Soc. Perkin Trans. 1* **1981**, 1630-1638.

(10) Garcia, C.; Malthête, J.; Collet, A. Key Intermediates in Cyclotriveratrylene Chemistry. Synthesis of New C3-cyclotriveratrylenes with Nitrogen Substituents. *Bull. Soc. Chim. Fr.*, **1993**, *130*, 93-95.

(11) Brotin, T.; Vanthuyne, N.; Cavagnat, D.; Ducasse, L., Buffeteau, T. Chiroptical Properties of Nona- and Dodecamethoxy Cryptophanes. *J. Org. Chem.* **2014**, *79*, 6028-6036.

(12) We use the following convention to describe the aza-compounds: The first stereo-descriptor is related to the oxygen-containing CTB unit and the second stereo-descriptor is related to the nitrogen-containing CTB unit.

(13) See for instance: a) Brotin, T.; Roy, V.; Dutasta, J.-P. Improved Synthesis of Functionals CTVs and Cryptophanes Using $Sc(OTf)_3$ as catalyst. *J. Org. Chem.* **2005**, *70*, 6187 - 6195. b) Long, A.; Jean. M.; Albalat, M.; Vanthuyne, N.; Giorgi, M.; Gorecki, M.; Dutasta, J.-P.; Martinez, A. Synthesis, Resolution, and Chiroptical Properties of Hemicryptophane cage Controlling the Chirality of Propeller Arrangement of a C_3 Triamide Unit. *Chirality*, **2019**, *31*, 910-916. c) Long, A.; Colomban, C.; Jean. M.; Albalat, M.; Vanthuyne, N.; Giorgi, M.; Di Bari, L.; Gorecki, M.; Dutasta, J.-P.; Martinez, A. Enantiopure C_1-Cyclotriveratrylene with a Reversed Spatial Arrangement of the Substituents. *Org. Lett.* **2019**, *21*, 160-165.

(14) Daugey, N.; Brotin, T.; Vanthuyne, N.; Cavagnat, D.; Buffeteau, T. Raman Optical Activity of Enantiopure Cryptophane. *J. Phys. Chem. B* **2014**, *118*, 5211-5217.

(15) Canceill, J.; Collet, A.; Gottarelli, G.; Palmieri, P. Synthesis and Exciton Optical Activity of D_3-Cryptophanes. *J. Am. Chem. Soc.* **1987**, *109*, 6454-6464.

(16) Taratula, O.; Hill, P. A.; Carroll, P. J.; Dmochowski, I. J. Crystallographic Observation of 'Induced Fit' in a Cryptophane Host-Guest Model System. *Nat. Commun.* **2010**, *148*, 1-7.

(17) Fogarty, H. A.; Berthault, P.; Brotin, T.; Huber, G.; Desvaux, H.; Dutasta, J.-P. A Cryptophane Core Optimized for Xenon Encapsulation. *J. Am. Chem. Soc.*, **2007**, *129*, 10332-10333.

(18) Spence, M. M.; Rubin, S. M.; Dimitrov, I. E.; Ruiz, J.; Wemmer, D.; Pines, A.; Yao, S. Q.; Tian, F.; Schultz, P. G. Functionalized Xenon as a Biosensor. *Proc. Natl. Acad. U.S.A*, **2001**, *98*, 10654-10657.

(19) Brotin, T.; Martinez, A.; Dutasta, J.-P. Water-Soluble Cryptophanes: Design and Properties. In *Calixarenes and Beyond*; Neri, P., Sessler, J. L., Wang, M.-X., Eds.; Springer International Publishing: Cham, **2016**; pp 525-557.

(20) a) Jayapaul, J.; Schröder; L. Molecular Sensing with Host Systems for Hyperpolarized 129Xe. *Molecules*, **2020**, *25*, 4627-4723. b) Mari, E.; Berthault, P. ^{129}Xe NMR Based Sensor: Biological Applications and Recent Methods. *Analyst*, **2017**, *142*, 3298-3308. c) Klippel, S.; Döpfert, J.; Jayapaul, J.; Kunth, M.; Rossella, F.; Schnurr, M.; Witt, C.; Freund, C.; Schröder, L. Cell Tracking with Caged Xenon: Using Cryptophanes as MRI Reporters Upon Cellular Internalization. *Angew. Chem.* **2014**, *126*, 503-506. d) Schröder, L. Xenon for NMR Biosensing – Inert but Alert. *Physica Medica*, **2013**, *29*, 3-16. e) Taratula, O.; Dmochowski, I. J. Functionalized ^{129}Xe Contrast Agents for Magnetic Resonance Imaging. *Current Opinion in Chemical Biology* **2010**, *14*, 97-104. f) Berthault, P.; Huber, G.; Desvaux, H. Biosensing Using Laser-Polarized Xenon NMR/MRI. *Progr. NMR Spectrosc.* **2009**, *55*, 35-60. g) Hilty, C.; Lowery, T. L. Wemmer, D. E.; Pines, A. Spectrally Resolved Magnetic Resonance Imaging of a Xenon Biosensor. *Angew. Chem. Int. Ed.* **2006**, *45*, 70-73.

(21) Schroder, L.; Lowery, T. J.; Hilty, C.; Wemmer, D.; Pines, A. Molecular Imaging Using a Targeted Magnetic Resonance Hyperpolarized Biosensor. *Science*, 2006, *314*, 446-449.

(22) Dubost, E.; Dognon, J.-P.; Rousseau, B.; Milanole, G.; Dugave, C.; Boulard, Y.; Léonce, E.; Boutin, C.; Berthault, P. Understanding a Host–Guest Model System through ^{129}Xe NMR Spectroscopic Experiments and Theoretical Studies. *Angew. Chem. Int. Ed.* 2014, *53*, 9837-9840.

(23) Chauvin, C. ; Liagre, L. ; Boutin, C. ; Mari, E. ; Léonce, E. ; Carret, G. ; Coltrinari, B. ; Berthault. P. Spin-Exchange Optical Pumping in a Van". Review of Scientific Instruments **87** (2016) 016105.

(24) a) Buffeteau, T.; Lagugné-Labarthet, F.; Sourrisseau, C. Vibrational Circular Dichroism in General Anisotropic Thin Solid Films: Measurement and Theoretical Approach. *Appl. Spectrosc.* **2005**, *59*, 732-745. b) Brotin, T.; Daugey, N.; Vanthuyne, N.; Jeanneau, E.; Ducasse, L., Buffeteau, T. Chiroptical Properties of Cryptophane-223 and -233 Investigated by ECD, VCD, and ROA Spectroscopy. *J. Phys. Chem. B* **2015**, *119*, 8631-8639.

(25) Frisch, M. J.; Trucks, G. W.; Schlegel, H. B.; Scuseria, G. E.; Robb, M. A.; Cheeseman, J. R.; Scalmani, G.; Barone, V.; Mennucci, B.; Petersson, G. A. et al. (see Supporting Information for full list of authors) *Gaussian 09*, revision A.1, Gaussian Inc., Wallingford CT, **2009**.